Expanded View Figures

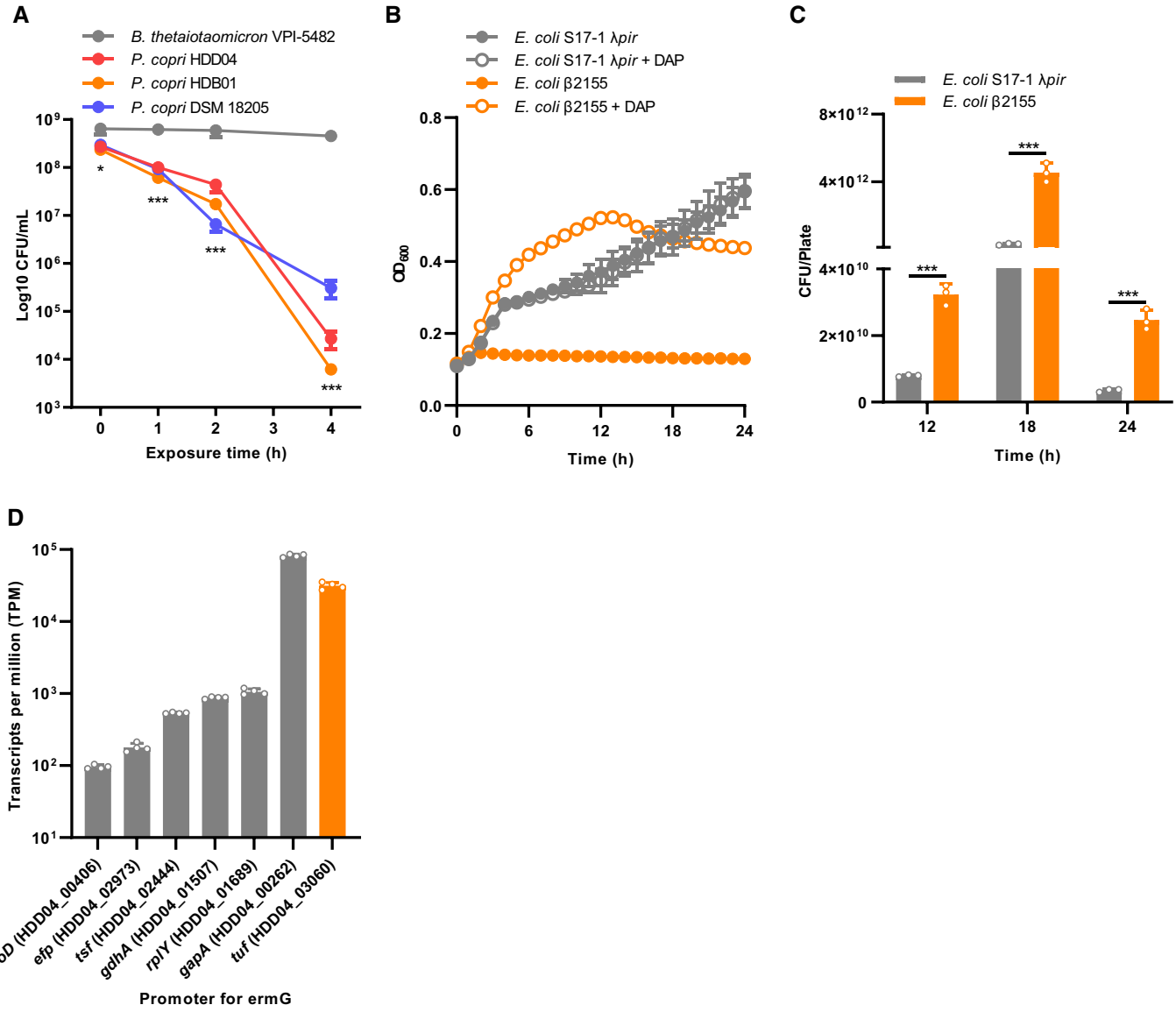

Figure EV1. Defining the impact of potential key factors on adapting conjugation system for *Prevotella copri*.

A Survival of *Bacteroides thetaiotaomicron* VPI-5482, *P. copri* HDD04, HDB01, and DSM 18205 in BHI + S broth in aerobic conditions. CFUs in the cultures were determined at indicated time points after exposure to normal air.

B Growth of *Escherichia coli* S17-1 λpir and *E. coli* β2155 in BHI + S broth in the presence or absence of diaminopimelic acid (DAP).

C Quantification of bacterial CFUs of *E. coli* S17-1 λpir and *E. coli* β2155 grown on BHI blood agar plates with DAP for three different time points.

D Transcription levels of seven genes in *P. copri* HDD04 grown in BHI + S broth. The promoter sequences of these genes were used for driving *ermG* expression in the plasmid in Fig 1D.

Data information: Values and error bars represent at least three biological replicates and their standard deviations (SDs), respectively. Asterisks indicate the significant differences (*$P < 0.05$; ***$P < 0.001$) calculated by Student's *t* test. In (A), asterisks represent the significant differences between *B. thetaiotaomicron* VPI-5482 and either one of three *P. copri* strains.

© 2021 The Authors

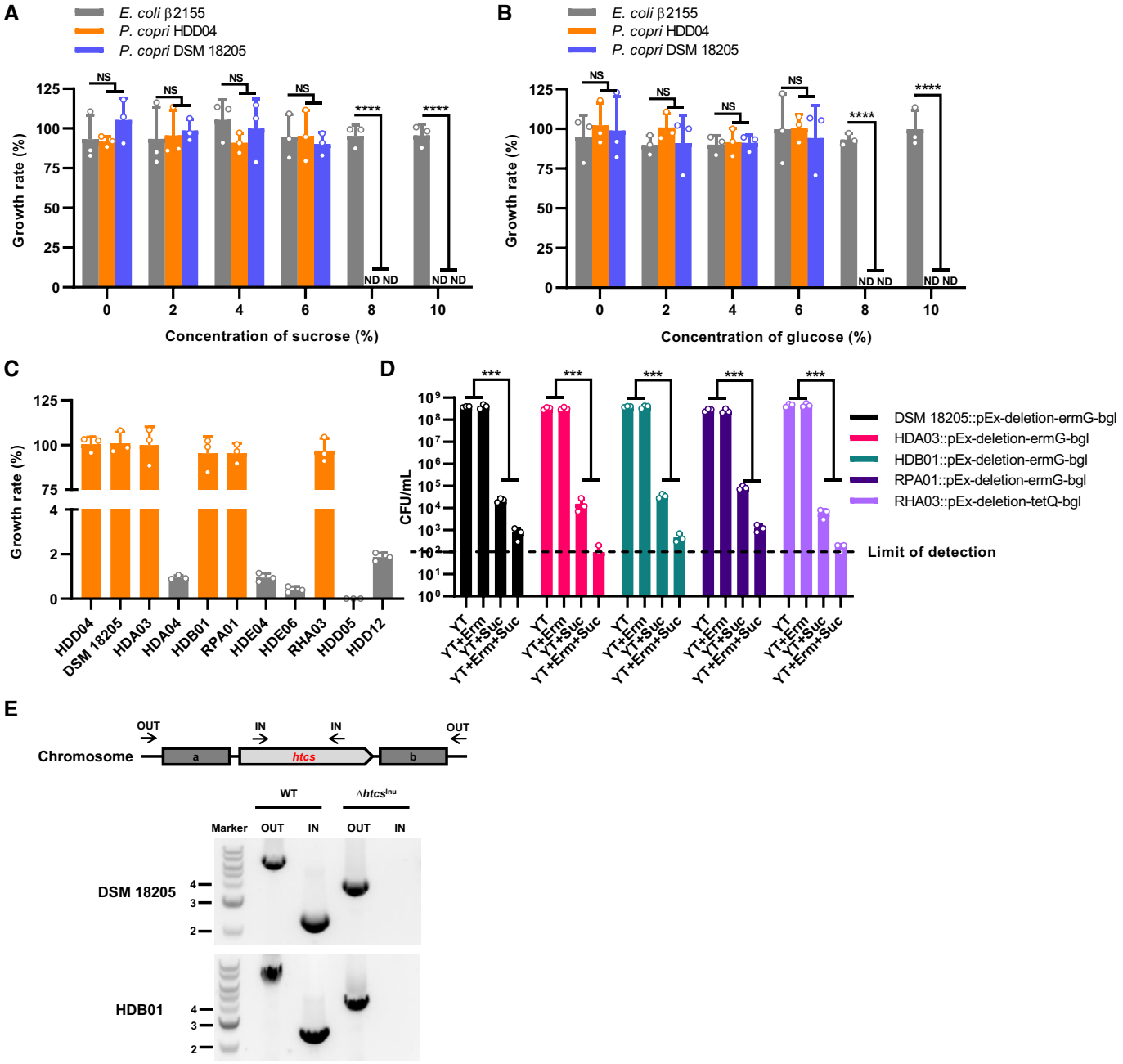

Figure EV2. Selectivity of *sacB*-based gene deletion system in *Prevotella copri*.

A, B Survival of *Escherichia coli* DH5α, *P. copri* HDD04 and DSM 18205 on agar plates supplemented with an increasing concentration of sucrose (A) or glucose (B). Serial dilutions of fresh *E. coli* β2155, *P. copri* HDD04 and DSM 18205 cultures were plated on YT or BHI + S agar plates with different concentrations of sucrose or glucose for counting CFUs. Growth rates were calculated by normalizing the CFU on YT + Sucrose/Glucose relative to BHI + S. ND: not detectable.

C Survival of *P. copri* strains grown on YT agar plates supplemented with 5% sucrose. Growth rates were calculated as described in (A). The gray color represents the inability of five strains in growing on YT + 5% sucrose.

D Viabilities of pEx-deletion integrated *P. copri* strains on agar plates with indicated supplements.

E Detection of gene deletion of the *htcs*^{Inu} homologs in *P. copri* HDB01 and DSM 18205. The up- and down-stream regions (dark gray) of the targeted gene and locations of primers ("OUT" and "IN", arrowheads) for PCR are indicated.

Data information: In (A–D), data shown are the mean of at least three biological replicates ± SD. Statistical significance between groups was calculated by Student's *t* test (***$P < 0.001$; and ****$P < 0.0001$; NS, $P > 0.05$, not statically significant).

© 2021 The Authors

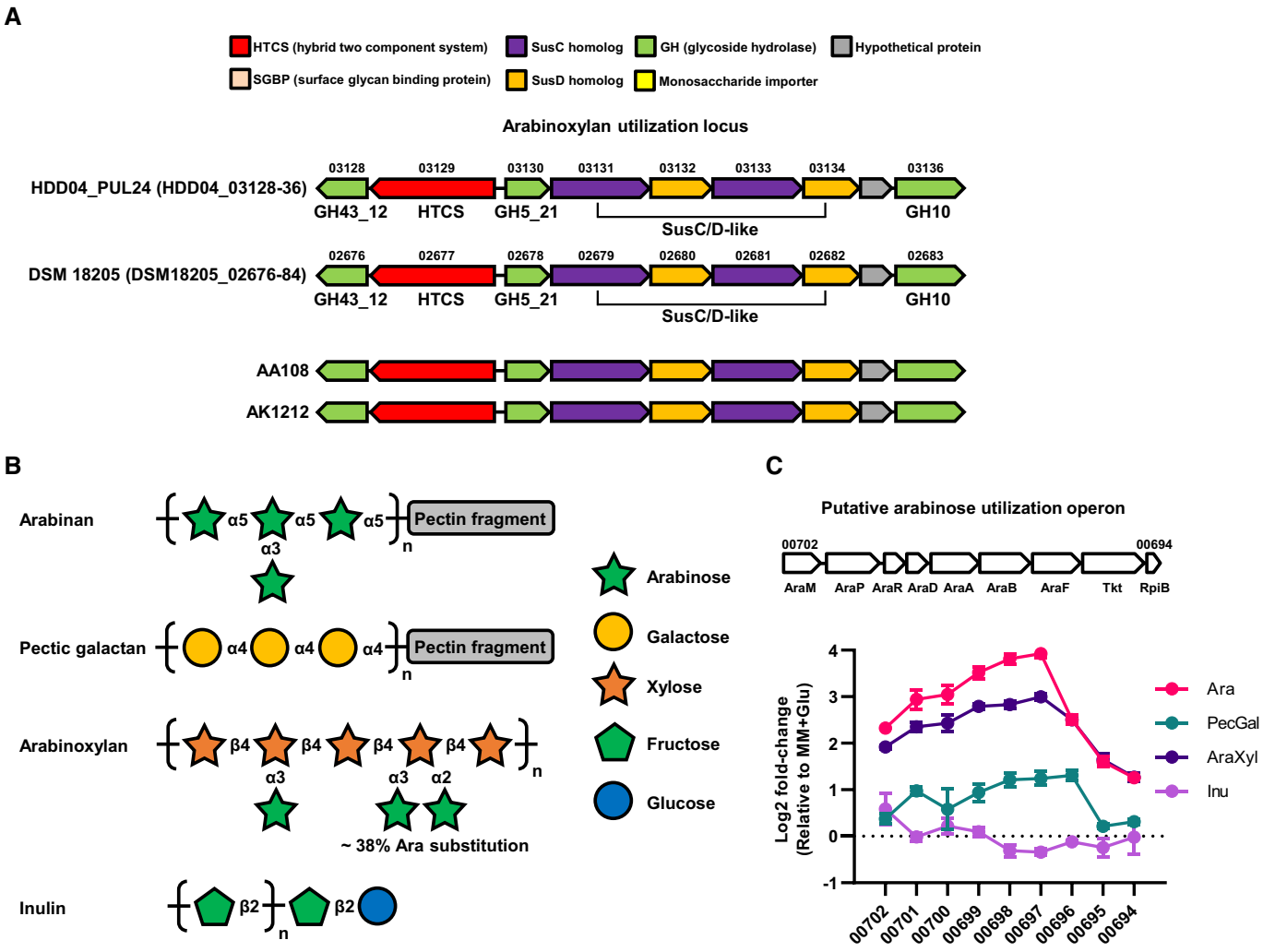

Figure EV3. Genetic and transcriptomic analysis of carbohydrate utilization by *Prevotella copri* strains.

A Gene organizations of homologous PUL^{AraXyl} in *P. copri* HDD04 and DSM 18205 in comparison with the predicted xylan utilization loci in two *P. copri* strains as described previously (Fehlner-Peach *et al*, 2019). Genes in PUL^{AraXyl} are annotated as described in Fig 4B.

B Graphic structures of arabinan, pectic galactan, arabinoxylan, and inulin used in this study. Different types of monosaccharides are represented according to "Symbol Nomenclature for Glycans" (https://www.ncbi.nlm.nih.gov/glycans/snfg.html). Detailed product information is provided on www.megazyme.com

C Gene composition of the putative arabinose utilization operon from HDD04 and expression levels of genes in this operon in MM supplemented with glucose or arabinan. For each dot, the average of transcription levels from three replicates are shown. The gene functions were predicted by BLAST on NCBI.

© 2021 The Authors

A

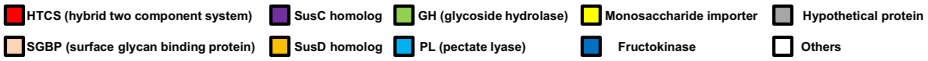

Clade	Strain	OD_{600} max	Organization of pectic galactan processing PUL
A	HDD04	0.8±0.05	
A	DSM18205	0.4±0.07	
A	HDA03	No growth	
A	HDA04	0.8±0.07	
A	HDB01	0.7±0.10	
A	HDC01	0.5±0.12	
A	RHA03	0.7±0.02	
A	RPA01	0.6±0.07	
C	HDE04	0.6±0.01	
C	HDE06	1.0±0.01	
D	HDD05	0.8±0.02	
E	HDD12	0.8±0.04	

B

Clade	Strain	OD_{600} max	Organization of arabinoxylan processing PUL
A	HDD04	0.7±0.03	
A	DSM18205	0.5±0.06	
A	HDA03	No growth	
A	HDA04	0.8±0.02	
A	HDB01	0.5±0.06	
A	HDC01	0.6±0.07	
A	RHA03	0.7±0.10	
A	RPA01	0.8±0.10	
C	HDE04	1.0±0.00	
C	HDE06	1.0±0.00	
D	HDD05	0.7±0.10	
E	HDD12	0.8±0.03	

C

Clade	Strain	OD_{600} max	Organization of inulin processing PUL
A	HDD04	0.7±0.02	
A	DSM18205	0.6±0.04	
A	HDA03	0.7±0.02	
A	HDA04	0.9±0.02	
A	HDB01	0.8±0.11	
A	HDC01	0.5±0.05	
A	RHA03	0.6±0.08	
A	RPA01	0.5±0.07	
C	HDE04	1.0±0.02	
C	HDE06	0.7±0.001	
D	HDD05	0.8±0.08	
E	HDD12	0.9±0.03	

Figure EV4. Gene organizations of PULs for processing pectic galactan, arabinoxylan, and inulin among multiple *Prevotella copri* strains with the capacities of growing on these polysaccharides.

A–C Gene organizations of PUL^{PecGal}, PUL^{AraXyl}, and PUL^{Inu} homologs among *P. copri* strains with distinct growth capacities on pectic galactan, arabinoxylan, and inulin, respectively. Maximum growth (OD_{600} max) of strains in MM supplemented with indicated polysaccharides is reported. Genes clustered in the PULs are displayed by arrows with different colors according to predicted functions of the gene products.

© 2021 The Authors

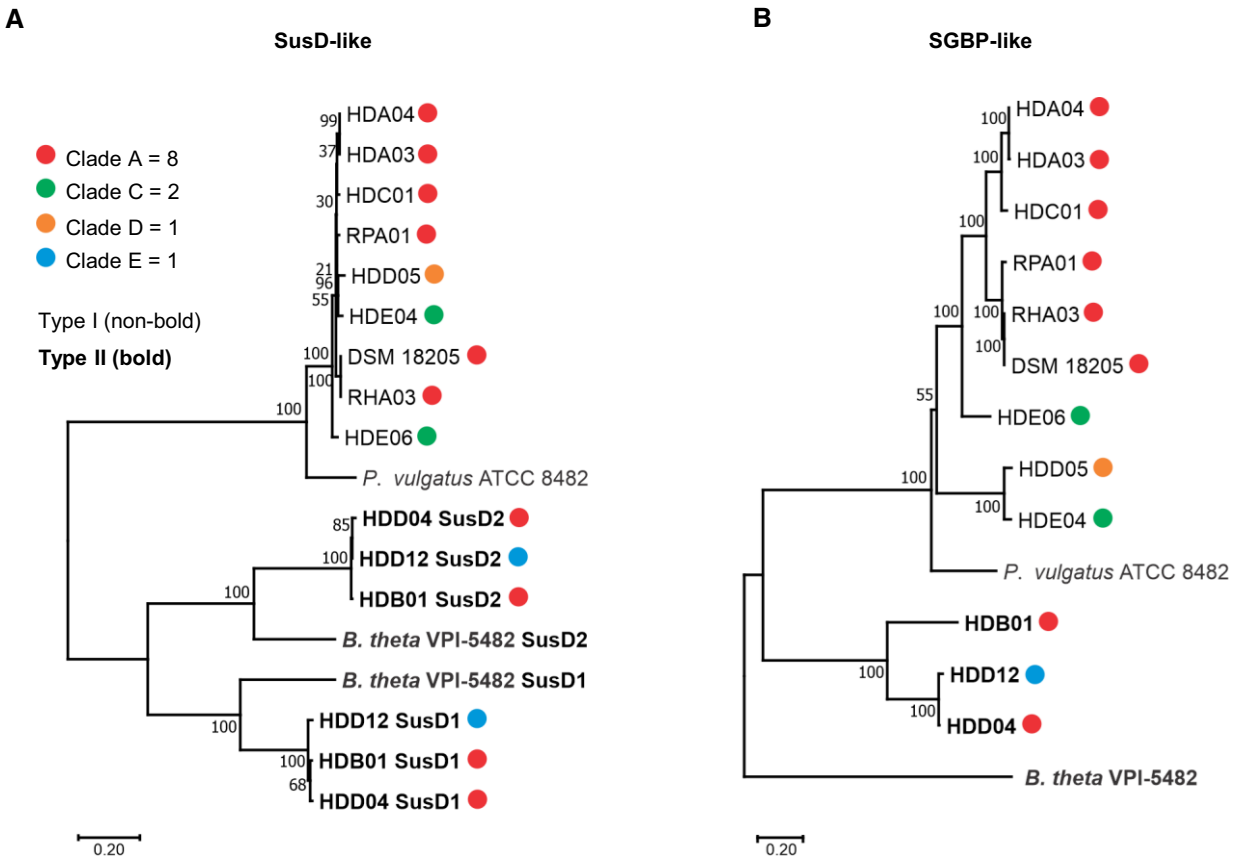

Figure EV5. Phylogenetic analysis of SusD-like and SGBP-like proteins encoded by two types of arabinan processing PULs.

A, B Phylogenetic trees of SusD-like (A) and SGBP-like (B) proteins of two types of arabinan processing PULs from *Prevotella copri* strains, *Bacteroides thetaiotaomicron VPI-5482*, and *Phocaeicola vulgatus* ATCC 8482. The strains from distinct *P. copri* clades are labeled by dots with different colors. The proteins from type-II PUL^{Ara} are shown in bold.

© 2021 The Authors